

A Multiple Resolution Study of Ka-Band HRR Polarimetric Signature Data

R.H. Giles^{*a}, W.T. Kersey^a, M.S. McFarlin^b, B.G. Woodruff^b, R. Finley^c, W.E. Nixon^d

^a University of Massachusetts Lowell, Submillimeter-Wave Technology Laboratory (STL)
175 Cabot Street, Lowell, Massachusetts 01854

^bSimulation Technologies (SimTech), Huntsville, AL 35898

^cTargets Management Office (TMO), Redstone Arsenal AL 35898

^dU.S. Army National Ground Intelligence Center (NGIC)
220 Seventh Street, N.E., Charlottesville, VA 22902

ABSTRACT

SAR resolution and polarization performance studies for ATR algorithms have been the source of recent attention. Thorough investigations are often hindered by the lack of rigorously consistent high-resolution full-polarimetric signature data for a sufficient number of targets across requisite viewing angles, articulations and environmental conditions. While some evaluative performance studies of high-value structures and conceptual radar systems may be effectively studied with limited field radar data, to minimize signature acquisition costs, pose-independent studies of ATR algorithms are best served by signature libraries fashioned to encompass the complexity of the collection scenario¹.

In response to the above requirements, the U.S. Army's National Ground Intelligence Center and Targets Management Office originated, sponsored, and directed a signature project plan to acquire multiple target signature data at Eglin, AFB using a high resolution full-polarimetric Ka-band radar². TMO and NGIC have sponsored researchers at both the Submillimeter-Wave Technology Laboratory and Simulation Technologies to analyze the trade-off between signature resolution and polarimetric features (ongoing research) of this turntable data. The signature data was acquired at five elevations spanning 5° to 60° for a T-72M1, T-72B, M1, M60-A3 and one classified vehicle. Using signal processing software established in an NGIC/STL-based signature study³, researchers executed an HRR and ISAR cross-correlation study involving multiple resolutions to evaluate peak performance levels and to effectively understand signature requirements through the variability of multiple target RCS characteristics.

The signature-to-signature variability quantified on the four unclassified MBTs is presented in this report, along with a description and examples of the signature analysis techniques exploited. This signature data is available from NGIC/TMO on request for Government Agencies and Government Contractors with an established need-to-know.

Key words: Millimeter, Polarimetric, Radar, Imagery, ATR, Correlation.

* Correspondence: Email: Robert_Giles@uml.edu; Telephone; (978) 458-3807; Fax: (978) 452-3333

Report Documentation Page				Form Approved OMB No. 0704-0188	
Public reporting burden for the collection of information is estimated to average 1 hour per response, including the time for reviewing instructions, searching existing data sources, gathering and maintaining the data needed, and completing and reviewing the collection of information. Send comments regarding this burden estimate or any other aspect of this collection of information, including suggestions for reducing this burden, to Washington Headquarters Services, Directorate for Information Operations and Reports, 1215 Jefferson Davis Highway, Suite 1204, Arlington VA 22202-4302. Respondents should be aware that notwithstanding any other provision of law, no person shall be subject to a penalty for failing to comply with a collection of information if it does not display a currently valid OMB control number.					
1. REPORT DATE AUG 2000		2. REPORT TYPE		3. DATES COVERED 00-00-2000 to 00-00-2000	
4. TITLE AND SUBTITLE A Multiple Resolution Study of Ka-Band HRR Polarimetric Signature Sata				5a. CONTRACT NUMBER	
				5b. GRANT NUMBER	
				5c. PROGRAM ELEMENT NUMBER	
6. AUTHOR(S)				5d. PROJECT NUMBER	
				5e. TASK NUMBER	
				5f. WORK UNIT NUMBER	
7. PERFORMING ORGANIZATION NAME(S) AND ADDRESS(ES) University of Massachusetts Lowell,Submillimeter-Wave Technology Laboratory,175 Cabot Street,Lowell,MA,01854				8. PERFORMING ORGANIZATION REPORT NUMBER	
9. SPONSORING/MONITORING AGENCY NAME(S) AND ADDRESS(ES)				10. SPONSOR/MONITOR'S ACRONYM(S)	
				11. SPONSOR/MONITOR'S REPORT NUMBER(S)	
12. DISTRIBUTION/AVAILABILITY STATEMENT Approved for public release; distribution unlimited					
13. SUPPLEMENTARY NOTES					
14. ABSTRACT					
15. SUBJECT TERMS					
16. SECURITY CLASSIFICATION OF:			17. LIMITATION OF ABSTRACT	18. NUMBER OF PAGES 10	19a. NAME OF RESPONSIBLE PERSON
a. REPORT unclassified	b. ABSTRACT unclassified	c. THIS PAGE unclassified			

1.0 THE MEASUREMENT FACILITY AND INSTRUMENTATION RADAR

The signature data was collected at the Eglin Air Force Base Seeker Test and Evaluation Facility (STEF) at Range C-52A. The STEF Millimeter Wave Instrumentation High Resolution Imaging Radar System (MIHRIRS) was used to collect the full-polarimetric signature data at Ka-band. The Ka-band radar system's characteristics are listed in Table 1.

Table 1. The Operational Parameters of the MIHRIRS Ka-band Polarimetric Radar

Parameter	Characteristic
Frequency	34.5 GHz (starting frequency)
RF Agile Bandwidth	1.024 GHz
Frequency Step Size	8 Mhz at 128 steps
Peak Power	7 watts
Pulse Width	50-100 nsec
PRF	50 KHz (max)
Beamwidth	7 degrees (two-way)
Gain	28.5 dB
Sidelobe level	27 dB down (min)
Polarization	full PSM linear (can also be circular)
Receiver IF Freq.	2.5-3.5 GHz
Receiver Matched Filter	12-24 MHz
SSB Receiver Noise Fig.	5 dB
Sensitivity	<-96 dBm

The STEF facility is equipped with a 300-foot tower, rail-mobile low RCS turntable, target loading berm, and target/turntable storage building. As shown in Figure 1, targets are positioned in range on a turntable that traverses along rails on asphalt in front of the tower. Changes are made in the elevation of the signature measurement by moving both the turntable and tower mounted radar. The signature data is calibrated by measuring simple shape reflectors mounted on concrete poles. See right photograph of Figure 2. Metal flashings are attached to the poles to minimize scattering contributions from the support structures. The calibration array on top of these structures is comprised of a 20 dBsm trihedral, 20 dBsm 45-degree gridded trihedral, 14 dBsm 0-degree dihedral and a 14 dBsm 45-degree dihedral. Measurement of these known reflectors with the full-polarimetric radar enables the operator to calculate both transmit and receive distortion matrices for the radar using the Barnes technique⁴.



Figure 1. The Eglin Air Force Base Seeker Test and Evaluation Facility (STEF) at Range C-52A



Figure 2. The Eglin Air Force Base Seeker Test and Evaluation Facility (STEF) at Range C-52A

Although several cables tether the 300' tower supporting the Ka-band radar, wind induced motion can adversely affect the turntable signature measurements by inducing a phase instability which causes blurring in target imagery. The effect is especially noticeable for steep elevations where the radar is positioned high on the 300' tower. If wind speeds were >12 knots, then the target data exhibits poor phase stability and the range would be shut down for the day. In some cases, the operations crew acquiring the radar data would identify the signature content (ISAR) as blurred, however sufficient for target exploitation. A motion compensation reflector was introduced to all target rotations in anticipation of tower motion problems with the signature data. Although the motion-comp reflector is placed in the target scene, the reflector is always outside the target range extent. For all tests, the reflector was positioned 15' behind the low RCS shroud/rail intersection (down-range) and 11' on the passenger side of the vehicle (cross range).

The motion compensation reflector is used as a phase reference between azimuth data samples during image formation. From one angle step to the next, the phase center for the motion compensation reflector is assumed constant. Thus any phase change in the range bin containing the motion-compensation reflector is due to wind induced tower/radar motion. A phase reference is established with the motion comp range bin for center azimuth sample and used to correct the phase over entire frequency ramps of adjacent azimuth samples within the image windows. Since the motion compensation reflector is not rotating with the target, the reflector will appear in the zero Doppler (or center) bin of the ISAR. If the reflector is positioned outside the target extent in slant range, then the reflector energy will not fold into the target. At high elevations care must be taken to consider the target extent. After motion compensation to the signature data is accomplished, the reflector is removed from the target scene through background subtraction.

The standard STEF MIHRIRS data delivery format is background subtracted. Background subtraction removes stationary clutter from target data, including the motion compensation reflector if present. Since motion compensation is not currently implemented in MIHRIRS software, all motion compensation as previously described must be applied through post-processing by the user. To enable this capability, the signature data for the MBT Requirements Analysis Program was delivered in both subtracted and unsubtracted formats for implementation of motion comp and background subtraction algorithms as desired.

2.0 THE CROSS-CORRELATION TECHNIQUES

The signature-to-signature RCS variability was quantified at three levels of dimensionality for the MBT turntable data acquired. Initially the raw complex radar return, $A(f, \alpha)$, as a function of frequency (f) and target angle (α) for the calibrated signature data contains the target of interest situated on a RAMed turntable. After motion compensation has been applied (if required), the back-scattered return other than from the target is removed using a cross-range clutter subtraction routine that exploits the target's rotational velocity. A total radar cross section (TRCS) signature-to-signature cross-correlation between target turntable measurements was executed as a first level RCS variability analysis. To perform this analysis the angular dependent (α) average TRCS (σ) for each target was computed at 1° increments by averaging the center frequency (f_c) back-scattered signal over 1° as shown in equation 2-1.

$$\sigma(\alpha) = 10 \log_{10} \{ \sum_{\alpha'=\alpha \pm 5^\circ} \| A_r(f_c, \alpha') \| \} \quad (2-1)$$

The signature-to-signature cross-correlation between two target turntable measurements was then quantified as an average difference (AD).

$$AD = 1/N_\alpha \sum_{\alpha \text{ over } 360^\circ} |\sigma_1(\alpha) - \sigma_2(\alpha \pm \delta\alpha)| \quad (\text{in units of dB}) \quad (2-2)$$

An angular adjustment ($\delta\alpha$) was implemented in equation 2-2 to minimize the AD and thus eliminate azimuth misalignment in the turntable signature data. The angle adjust values calculated for this signature set are reflected in Table 1.

As the second level RCS variability analysis of the MBT turntable signature data, high-resolution range (HRR) profiles were formed through application of a Hanning Window (H_f) along with execution of a fast Fourier transform in frequency (F_f) generating angular dependent complex target profiles, equation 2-3.

$$A_r(\alpha) = F_f \{ H_f [A(f, \alpha)] \} \quad (2-3)$$

The cross-correlation could then be executed between HRR RCS Profiles by performing an angular average over $\approx 0.4^\circ$ as depicted in equation 2-4.

$$\sigma_r(\alpha) = 10 \log_{10} \{ \sum_{\alpha'=\alpha \pm 2^\circ} \| A_r(\alpha') \| \} \quad (\text{in units of dBsm}) \quad (2-4)$$

To insure that the cross-correlation levels calculated represents differences between target scattering features and not the surrounding terrain, an angular dependent clutter separation threshold (CST) was established as the mean of the HRR RCS profile, equation 2-5.

$$\sigma(\alpha) = 1/N_r \{ \sum_r \sigma_r(\alpha) \} \quad (2-5)$$

Then, for $\sigma_{r1}(\alpha)$ or $\sigma_{r2}(\alpha)$ greater than the CST $\sigma(\alpha)$, the signature-to-signature cross-correlation between two target turntable measurements was quantified as an average percent difference APD in equation 2-6.

$$APD = 1/(N_\alpha N_r) \sum_r \sum_\alpha |\sigma_{r1}(\alpha) - \sigma_{r2}(\alpha')| / [\sigma_{r1}(\alpha) + \sigma_{r2}(\alpha') + 2|\sigma(\alpha)|] \times 100\% \quad (2-6)$$

The azimuth and range of the second target $\alpha' = \alpha \pm \delta\alpha$ and $r_2 = r_1 \pm \delta r$ were defined as variables relative to the first target for performing the positional adjustments in the HRR profile minimizing the HRR APD and eliminating error contributions due to target alignment. The RCS gain was also adjusted for one target relative to the second, with no positive change observed. This is a strong indication of well-calibrated signature data.

An algorithm similar to equation 2-6 was implemented for the high resolution ISAR imagery at 1° aspect increments for the entire spin of the target. The range and cross-range of the second target $r_2 = r_1 \pm \delta r$ and $cr_2 = cr_1 \pm \delta cr$ were defined as variables relative to the first target for performing the positional adjustments in the ISAR minimizing the imagery's APD and eliminating error contributions due to image alignment. The target's alignment in azimuth was corrected using the angular adjustment calculated during execution of the TRCS comparative method, equation 2-2. Since the data was determined to be well calibrated, no adjustment in the RCS gain was made.

3.0 THE SIGNATURE DATA AND ANALYSIS

The high-resolution full-polarimetric Ka-Band turntable signatures of the MBTs were acquired over a two-week period in April of 1999. The signature data was acquired at five elevations spanning 5° to 60° for a T-72M1, T-72B, M1, M60-A3 and one classified vehicle. Shown in Table 1 is the sequence of signature measurements performed on the unclassified vehicles. Measurements at a single elevation were acquired consecutively within a day. Signatures were acquired on the T-72/M1, twice at several elevations, to establish a baseline of measurement variability for a single target. As the first and last measurement for each day along with two consecutive measurements on day two, the T-72M1 signature data provides ample evidence of the system performance.

Table 1. The sequence of MBT signature data acquired at the Eglin Air Force Base Seeker Test and Evaluation Facility

Run #	Date	File Desig.	Elevation	Target	Sweep Count	Aspect Adjust
4	4/19/99	6715	5	T-72M1	38314	3.2
6	"	6717	5	T-72B	37982	3.6
7	"	6722	5	M60	38032	3.8
8	"	6723	5	M1 basic	38074	1.4
9	"	6724	5	T-72M1	38097	2.0
10	4/20/99	6734	15	T-72M1	38850	3.2
11	"	6735	15	T-72M1	38758	3.2
13	"	6741	15	T-72B	37883	4.4
14	"	6742	15	M-60	37816	4.6
15	"	6743	15	M1 basic	37718	4.4
16	4/21/99	6752	30	T-72M1	38453	3.9
17	"	6753	30	T-72B	38027	3.3
18	"	6754	30	M-60	37580	3.4
19	"	6759	30	M1 basic	37379	4.7
21	"	6761	30	T-72M1	37396	2.4
22	4/22/99	6770	45	T-72M1	38007	2.5
26	4/26/99	6782	45	T-72B	37263	3.6
27	"	6783	45	M-60	38003	2.5
29	"	6785	45	M1 basic	37809	3.2
30	"	6786	45	T-72M1	37743	2.4
31	4/27/99	6795	60	T-72M1	38465	1.0
32	4/28/99	6800	60	T-72M1	38822	0.4
33	"	6801	60	T-72B	38237	2.1
37	4/29/99	6813	60	M1 basic	39041	0.5
38	"	6814	60	M-60	38562	1.0

Six, twelve and twenty four inch resolution ISAR imagery was generated at 1° aspect increments for the entire spin of each target. Using the spatial average of the percent difference between VV amplitude images (in units of dBsm) for the 360 ISARs as described in Section 2.0, an APD was calculated for all combinations of targets at each elevation. The cross-correlation between VV ISAR imagery of targets at two of the five elevations for three different spatial resolutions, has been documented in Tables 2 through 7. There was satisfaction in the observation that the cross-correlation values between the two measurements on the reference T-72/M1 are consistently the lowest tabulated value at every elevation. In fact the value for the two measurements performed consecutively on the T-72, without removing the vehicle from the turntable, exhibited the highest correlation (lowest values). See Tables 5 through 7. The higher correlation between individual measurements of the T-72M1 is the first indication that there are statistically measurable differences in the signatures between targets using the ISAR imagery.

At low elevations, the largest statistical differences in imagery between the four MBTs consistently occurred for the M1. In hindsight, this result is not surprising given the unique physical differences of the M1 from other MBTs. The M1 consists only of large clean sections of flat plate armor with little or no tools or other items strapped externally to the hull to provide multiple unusual scattering geometries. With knowledge of the standard deviation for each correlation value, one may make the observation that while the measurements consistently stack with the T-72B correlating best with the T-72M1, statistically only imagery measurements at resolutions better than 2' enable one to separate ISAR of the same MBT from another. Tables 2, 3 and 4 for the 5° elevation signature data have been depicted graphically in Figure 3 to illustrate the impact of image resolution on the ISAR correlation algorithm. Figure 4 demonstrates that at resolutions better than 2', the ISAR imagery is separable from any two of the MBTs for which signatures were acquired.

Table 2. The cross-correlation of 6'' resolution VV ISAR for four main battle tanks at 5° elevation.

T-72		T-72		T-72 B		M 60	
% Diff	Std.	% Diff	Std.	% Diff	Std.	% Diff	Std.
T-72	6.0	0.5	T-72	7.6	0.6	T-72 B	
T-72 B	7.8	0.6	T-72 B	8.0	0.6	M 60	
M 60	8.5	0.6	M 60	8.3	0.6	M 1	
M 1	9.1	0.7	M 1				

Table 3. The cross-correlation of 12'' resolution VV ISAR for four main battle tanks at 5° elevation.

T-72		T-72		T-72 B		M 60	
% Diff	Std.	% Diff	Std.	% Diff	Std.	% Diff	Std.
T-72	6.0	0.7	T-72	7.1	0.7	T-72 B	
T-72 B	7.3	0.7	T-72 B	7.0	0.7	M 60	
M 60	7.8	0.8	M 60			M 1	
M 1	8.2	0.8	M 1				

Table 4. The cross-correlation of 24'' resolution VV ISAR for four main battle tanks at 5° elevation.

T-72		T-72		T-72 B		M 60	
% Diff	Std.	% Diff	Std.	% Diff	Std.	% Diff	Std.
T-72	5.6	0.9	T-72	6.1	0.8	T-72 B	
T-72 B	6.5	0.9	T-72 B	5.9	0.9	M 60	
M 60	6.9	0.9	M 60	6.1	1.0	M 1	
M 1	6.9	1.1	M 1				

Table 5. The cross-correlation of 6'' resolution VV ISAR for four main battle tanks at 15° elevation.

T-72		T-72		T-72 B		M 60	
% Diff	STD	% Diff	STD	% Diff	STD	% Diff	STD
T-72	2.4	0.8	T-72	8.1	0.6	T-72 B	
T-72 B	7.5	0.5	T-72 B	8.5	0.7	M 60	
M 60	8.4	0.5	M 60	8.5	0.7	M 1	
M 1	8.9	0.7	M 1				

Table 6. The cross-correlation of 12'' resolution VV ISAR for four main battle tanks at 15° elevation.

T-72		T-72		T-72 B		M 60	
% Diff	Std.	% Diff	Std.	% Diff	Std.	% Diff	Std.
T-72	3.3	1.1	T-72	7.2	0.7	T-72 B	
T-72 B	6.9	0.6	T-72 B	7.4	0.8	M 60	
M 60	7.8	0.8	M 60			M 1	
M 1	8.1	0.8	M 1				

Table 7. The cross-correlation of 24'' resolution VV ISAR for four main battle tanks at 15° elevation.

T-72		T-72		T-72 B		M 60	
% Diff	Std.	% Diff	Std.	% Diff	Std.	% Diff	Std.
T-72	4.0	1.2	T-72	6.0	1.2	T-72 B	
T-72 B	6.0	0.9	T-72 B	6.1	1.0	M 60	
M 60	6.7	1.0	M 60			M 1	
M 1	6.9	1.2	M 1				

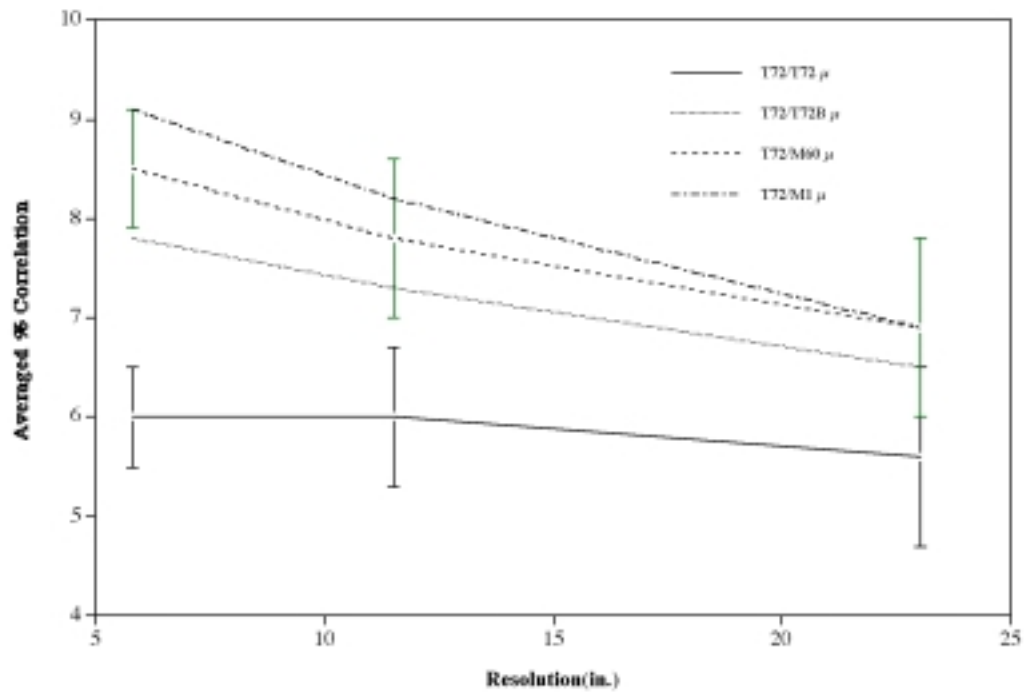


Figure 3. The cross-correlation of VV ISAR as a function of image resolution for a T-72 against an independent spin of the T-72 and three other main battle tanks.

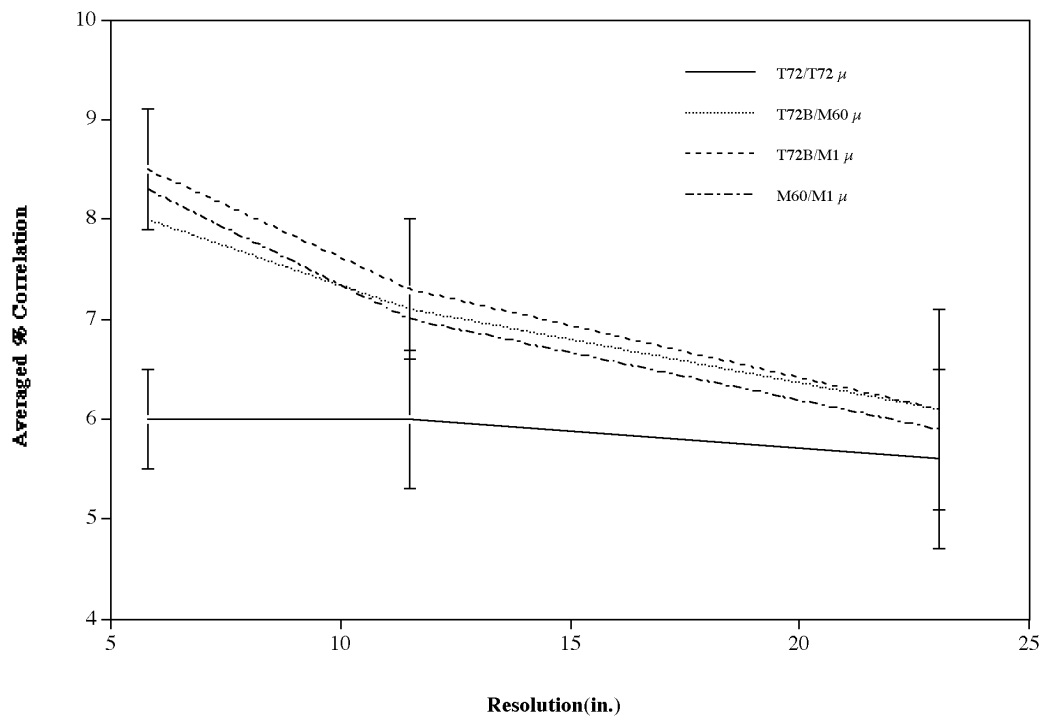


Figure 4. The VV ISAR cross-correlation between two turntable measurements of a T-72 as compared to the cross-correlation of three other main battle tanks.

Table 8. The cross-correlation of 6'' resolution VV RCS range profiles for four main battle tanks at 5° elevation.

	T-72			T-72			T-72 B			M-60	
	% Diff	Std.		% Diff	Std.		% Diff	Std.		% Diff	Std.
T-72	5.0	1.2									
T-72 B	6.8	1.7		6.4	1.7						
M 60	7.7	2.1		7.2	2.1		7.0	2.0			
M 1	8.6	2.5		7.9	2.4		7.3	2.0		7.3	2.2

Table 9. The cross-correlation of 12'' resolution VV RCS range profiles for four main battle tanks at 5° elevation.

	T-72			T-72			T-72 B			M-60	
	% Diff	Std.		% Diff	Std.		% Diff	Std.		% Diff	Std.
T-72	4.7	1.4									
T-72 B	6.3	2.0		6.0	1.8						
M 60	7.1	2.2		6.7	2.1		6.3	1.9			
M 1	7.8	2.6		7.4	2.4		6.7	2.0		6.7	2.3

Table 10. The cross-correlation of 24'' resolution VV RCS range profiles for four main battle tanks at 5° elevation.

	T-72			T-72			T-72 B			M-60	
	% Diff	Std.		% Diff	Std.		% Diff	Std.		% Diff	Std.
T-72	4.7	1.7									
T-72 B	6.1	2.1		5.9	1.9						
M 60	7.2	2.4		6.6	2.2		6.0	2.1			
M 1	7.7	3.0		7.2	2.7		6.5	2.2		6.5	2.3

Table 11. The cross-correlation of 6'' resolution VV RCS range profiles for four main battle tanks at 15° elevation.

	T-72			T-72			T-72 B			M-60	
	% Diff	Std.		% Diff	Std.		% Diff	Std.		% Diff	Std.
T-72	1.7	0.8									
T-72 B	7.1	1.8		7.0	1.8						
M 60	8.4	2.3		8.4	2.3		8.2	2.4			
M 1	8.0	2.1		8.1	2.2		8.4	2.2		8.3	2.1

Table 12. The cross-correlation of 12'' resolution VV RCS range profiles for four main battle tanks at 15° elevation.

	T-72			T-72			T-72 B			M-60	
	% Diff	Std.		% Diff	Std.		% Diff	Std.		% Diff	Std.
T-72	2.0	0.9									
T-72 B	6.5	1.9		6.5	1.9						
M 60	8.0	2.5		8.2	2.6		7.8	2.6			
M 1	7.4	2.3		7.6	2.4		7.6	2.4		7.6	2.4

Table 13. The cross-correlation of 24'' resolution VV RCS range profiles for four main battle tanks at 15° elevation.

	T-72			T-72			T-72 B			M-60	
	% Diff	Std.		% Diff	Std.		% Diff	Std.		% Diff	Std.
T-72	2.3	1.1									
T-72 B	6.2	2.0		6.3	2.1						
M 60	8.0	2.8		8.3	2.9		7.6	2.7			
M 1	7.4	2.9		7.6	3.1		7.2	2.6		7.5	2.6

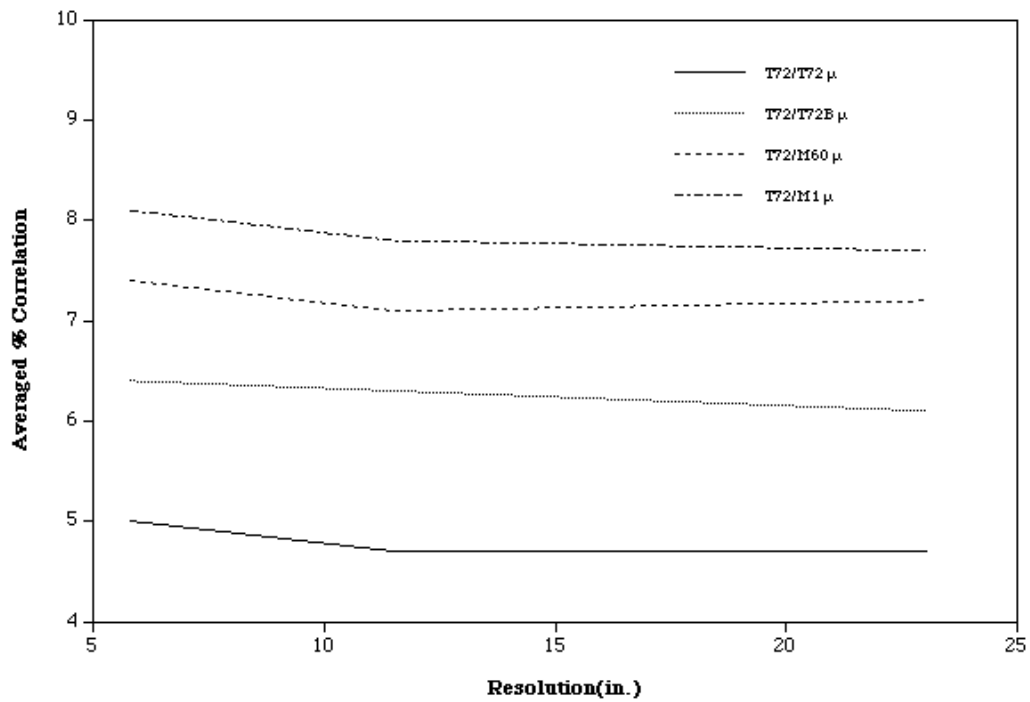


Figure 5. The cross-correlation of aspect averaged VV range profiles as a function of range resolution for a T-72 against an independent spin of the T-72 and three other main battle tanks.

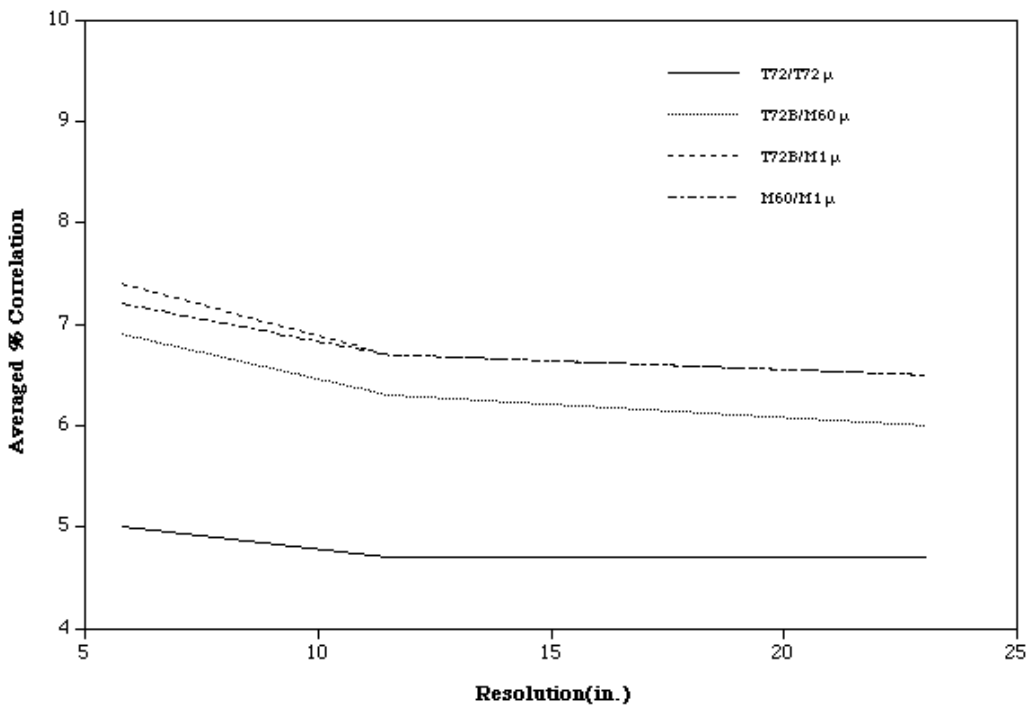


Figure 6. The cross-correlation of aspect averaged VV range profiles as a function of range resolution between two turntable measurements of a T-72 as compared to the cross-correlation of three other main battle tanks.

Six, twelve and twenty four-inch resolution aspect averaged RCS range profiles were generated at 1° aspect increments for the entire spin of each target. Using the range profiles, which were acquired at an aspect resolution of $\approx 0.0097^\circ$, a 40 point linear average in target aspect was executed to create the 360 high range resolution (HRR) profiles for the correlation study. Using Equation 2-6, an APD was calculated for all combinations of targets at each elevation. The cross-correlation between VV RCS profiles of targets at two of the five elevations for three different spatial resolutions, has been documented in Tables 8 through 13. As with the correlation results of the ISAR imagery, there was satisfaction in the observation that the cross-correlation values between the two measurements on the reference T-72/M1 are consistently the lowest tabulated value at every elevation. The value for the two measurements performed consecutively on the T-72, without removing the vehicle from the turntable, exhibited the highest correlation (lowest values) just as with the ISAR. See Tables 11 through 13.

The larger standard deviation reflected in Tables 8 through 13 (as compared to the corresponding ISAR correlation values), one realizes that the higher correlation between individual measurements of the T-72M1 are insufficient to generate statistically measurable differences in the signatures between targets using the HRR profiles only. No error bars reflecting the standard deviation for correlation of the range profiles were depicted in Figures 5 and 6 since they would extend beyond the graphical representations. The loss of dimensionality in cross-range has more than doubled the standard deviation as the mean values have come together. Separability between MBTs using range profile only, even at 6" resolution, appears difficult using the correlation metrics exploited. The driving feature for this range only correlation algorithm appears to be spatial extent of the profiles, not persistence of the bin-to-bin amplitudes. Additional features such as the full polarimetric nature of the signature data have also been initiated with these correlation algorithms using the HRR profiles only. While separability between the MBTs improved, no arguments could be made at this time about advantages based on the methodologies implemented. Enhancements are being made to the correlation algorithms expressed in Section 2.0 to accurately definitize the advantages of exploiting the full polarimetric nature of this signature data.

4.0 CONCLUSIONS

The impact of resolution on the correlation of signatures between four main battle tanks (MBTs) has been explored for ISAR imagery, HRR RCS profiles and TRCS signature data. Confidence in the metrics and signature data exploited was quantified through ISAR and HRR cross-correlation values between the multiple measurements of a T-72/M1. While target separability seems easily achievable between these four MBTs using 6" resolution ISAR, the difficulty of exploiting lower resolution MMW ISAR or HRR profiles has been made evident. When bin-to-bin isolation of a target's scattering features is not achieved through signature dimensionality and resolution, only spatial extent appears to drive the cross-correlation of these images and range profiles.

The signature data acquired in this measurements program is available from NGIC/TMO on request for Government Agencies and Government Contractors with an established need-to-know.

5.0 REFERENCES

1. L.M. Novak, S.D. Haversen, G.J. Owirka, and M. Hiatt, "Effects of Polarization and Resolution on the Performance of a SAR ATR System", MIT Lincoln Laboratory Journal, Vol. 8, No. 1, pp. 49-67, Spring/Summer 1995.
2. R. Finley, M.S. McFarlin, B.G. Woodruff, R.H. Giles, and W.E. Nixon, "Main Battle Tank (MBT) Requirements Analysis", Targets Management Office Final Report, March 2000
3. W.E. Nixon, W. T. Kersey, L. C. Perkins and R.H. Giles, "A Variability Study of Ka-Band HRR Polarimetric Signatures on Eleven T-72 Tanks", SPIE proceedings of the 12th Annual International Symposium on Aerospace/Defense Sensing, Simulation, and Controls, April 1998.
4. Barnes, R.M., "Polarization Calibration Using In-Scene Reflectors", Project Report TT-65, MIT Lincoln Laboratory, 10 September 1986